

Copyright is owned by the Author of the thesis. Permission is given for a copy to be downloaded by an individual for the purpose of research and private study only. The thesis may not be reproduced elsewhere without the permission of the Author.

**THE EFFECT OF ADDED CO-SOLVENT ON THE PHASE  
BEHAVIOUR OF THE MICELLAR LIQUID CRYSTAL SYSTEM  
CAESIUM PENTADEC AFLUORO OCTANOATE / WATER.**

A thesis presented in partial fulfilment of the requirements for the degree of  
Master of Science in Chemistry at Massey University.

**Scott Jonathan Thomsen**

**1994**

## **Acknowledgements.**

My sincere thanks go to my supervisor, Associate Professor Ken Jolley for his encouragement, guidance, and patience.

My thanks also go to Dr Ashok Parbhu for his invaluable contribution to this work.

Special thanks go to my parents, Neville and Jennifer Thomsen, Elsthorpe.

## Abstract

The effect of the addition of the co-solvents formamide (FA), *N*-methylformamide (NMF), *N,N*-dimethylformamide (DMF), and *N,N*-dimethylacetamide (DMA) on the phase behaviour of the micellar liquid crystal system caesium pentadecafluorooctanoate (CsPFO)/D<sub>2</sub>O (weight fraction CsPFO=0.5) has been determined. In all cases the effect of the addition of co-solvent is to decrease the isotropic (I)-to-nematic ( $N_D^+$ ) and the nematic - to - lamellar ( $L_D$ ) phase transition temperatures. At a co-solvent mole fraction of 0.01 the observed decreases in the I-to- $N_D^+$  phase transition temperatures ( $T_{NI}$ ) were 5.3 K, 15.5 K, 15.7 K, and 18.8 K for the co-solvents FA, NMF, DMF, and DMA respectively, whilst the corresponding decrease for the  $N_D^+$ -to- $L_D$  phase transition temperatures ( $T_{NL}$ ) were 5.5 K, 16.1 K, 16.3 K, and 19.1 K. Thus, at low co-solvent concentrations, the main effect is simply to displace the phase transition lines to lower temperatures and there is no significant change in the overall phase behaviour other than a small increase in the temperature range of the  $N_D^+$  phase. <sup>2</sup>H NMR measurements reveal that, in all cases, increasing the co-solvent concentration at constant temperature results in concomitant decreases in micelle aggregation numbers but the micelle sizes at  $T_{NI}$  and those at  $T_{LN}$  are essentially the same, i.e. the phase transitions are determined by hard particle interactions. Thus, the effect of co-solvent on the phase behaviour can be understood in terms of changes in micelle self-assembly, with addition of co-solvent shifting the distribution of micelle sizes to a lower mean aggregation number and decrease in temperature shifting the distribution of micelle sizes to a higher one. NMF, DMF, and DMA have a much greater effect on micelle size distribution than does FA.

## Table of Contents.

1. Introduction. ....	1
2. Experimental. ....	4
2.1. Chemicals. ....	4
2.2. Sample Preparation. ....	4
2.2.1 NMR Sample Preparation. ....	4
2.2.2 Conductivity Sample Preparation. ....	5
2.3. Instrumentation. ....	5
2.3.1 Temperature control. ....	5
2.3.2 Temperature Measurement. ....	7
2.3.3 NMR Instrumentation. ....	8
2.3.4 Conductivity Instrumentation. ....	9
3. NMR Theory. ....	10
3.1. Quadrupole Energies For Nuclei With $I > 1/2$ . ....	11
3.1.1 $^2\text{H}$ ( $I=1$ ) ....	14
3.1.2 $^{133}\text{Cs}$ ( $I=7/2$ ) ....	15
3.2. $^{133}\text{Cs}$ Chemical Shift Anisotropies. ....	15
4. The Effect of Co-Solvent on Liquid Crystal Phase Behaviour. ....	17
4.1. Phase Diagrams. ....	17
4.2. Phase Identification and Determination of Phase Transition Temperatures. ....	22
4.2.1 Phase Characterisation. ....	22
4.2.1.1 $^2\text{H}$ NMR Spectra. ....	22
4.2.1.2 $^{133}\text{Cs}$ NMR spectra. ....	24
4.2.2 Determining Phase Transition Temperatures. ....	24
4.2.2.1 Determining $T_{IN}$ . ....	27
4.2.2.2 Determining $T_{NI}$ . ....	28
4.2.2.3 Determining $T_{NL}$ & $T_{LN}$ . ....	28
4.3. The Effect of Co-solvent on Micelle Size. ....	35
4.3.1 Introduction. ....	35
4.3.2 Variation of Micelle Size with Temperature. ....	36
4.3.3 Variation of Micelle Size with Co-solvent. ....	36
4.3.4 Variation of Micelle Size along the Phase Transition Lines. ....	37
4.3.5 Micelle Size and Bound-ion Fraction $\beta$ . ....	37
4.3.6 Summary. ....	38
5. The Effect of Cosolvent on Self-Assembly in dilute CsPFO/ $\text{D}_2\text{O}$ Solutions. ....	43
5.1. Self-Assembly. ....	43
5.2. Measurement of CMC's. ....	46
5.3. CMC Results. ....	46
6. Discussion. ....	49
6.1. Nature of I/N and N/L transitions in the binary systems. ....	49
6.2. Self Assembly of the Micelles in the Ternary Systems. ....	49
6.3. Conclusions. ....	54
Appendix 1. Phase Transition Temperatures. ....	56
Appendix 2. Hazard Sheet. ....	57
References. ....	58

## 1. Introduction.

Short chain perfluorocarbon carboxylic acids are exceptional for their preference to form solutions of discotic micelles which are stable over wide concentration and temperature intervals. This results in generic phase behaviour<sup>1-3</sup> in which the discotic micelles, with increasing concentration, undergo a sequence of disorder-order transitions to form first a nematic phase and, subsequently, a smectic lamellar phase<sup>4,5</sup>. The nematic phase  $N_D^+$  is characterised by long-range correlations in the orientation of the symmetry axes of the micelles, whilst in the dilute lamellar phase  $L_D$  the micelles are arranged on equidistant planes.

The origin of the stability of discotic micelles is not currently understood, indeed simple statistical mechanical models suggest that they are intrinsically unstable and should undergo spontaneous growth to form infinite bilayers as is the case for phospholipids for example<sup>6</sup>. The existence of discotic micelles is now universally expected, however, and theoretical models have been proposed to account for their intrinsic stability. Within the framework of the McMullen model<sup>7,8</sup>, the micelle is taken to be an oblate right-circular cylinder (body) closed by a half-toroidal rim. The chemical potential of a surfactant molecule will clearly be different in the “body” than in the “rim”. It has been shown that only small discotic micelles can be stable, and this requires that the chemical potential of the surfactant in the rim be slightly greater than in the body so that the entropy of mixing off-sets their explosive growth into infinite bilayers.

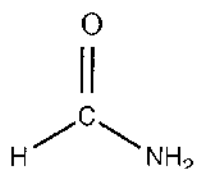
Discotic nematic phases are found intermediate to isotropic micellar solutions at high temperatures/low concentrations and a smectic (lamellar) phase at lower temperatures/higher concentrations. They appear to be stable within the concentration interval about 0.1 to 0.5 volume fraction of amphiphile. Across this concentration interval the axial ratio  $a/b$ , where  $a$  is the length of the major, or symmetry axis and  $b$  the length of the two equivalent minor perpendicular axes, is typically in the range 0.25 to 0.5 for disc-shaped micelles and the maximum dimension of the micelle is of the order of the separation of the centres-of-mass. Thus, an Onsager type<sup>9</sup> description of the nematic order seems appropriate. For flat discs of depth  $d$  and diameter  $\sigma$  the volume fractions in the co-existing isotropic and nematic phases are:  $\phi_i=2.97d/\sigma$  and  $\phi_n=3.20d/\sigma$ <sup>10,11</sup>. For particles with smaller anisotropies computer simulations<sup>12-14</sup> of hard ellipsoids have established that nematic states exist from  $a/b < 1/2.75$  for oblate ellipsoids. Theoretical treatments<sup>15</sup> have established the relation between  $\phi_{i,n}$  and  $a/b$  for these small ellipsoids making comparison with experiment practicable: for oblate ellipsoids with  $a/b = 1/5$ ,  $\phi_i = 1.67ab$  and  $\phi_n = 1.80ab$ . Computer simulations on cut spheres<sup>16</sup> defined by a length-to-width ratio  $L/D$ , where  $D$  is the sphere diameter and  $L$

( $<D$ ) is the distance between the parallel flat surfaces, reveal a transition from a nematic phase to a translationally ordered columnar phase at higher densities for  $L/D = 0.1$ . However, the inherent distribution in size of the aggregates in micellar nematic phases is expected to significantly affect the structure of any translationally ordered phases which occur<sup>17</sup>. The micelle sizes are expected to vary with concentration and temperature and to depend upon the nature of the forces between the micelles and also upon any coupling to the symmetry and order of the mesophase. This will have a marked effect on the phase behaviour. Thus, any theory of micellar nematic phases must include the self-assembly behaviour of surfactants in aqueous solution. Taylor and Herzfeld<sup>18</sup> have considered liquid crystal phases formed in reversibly self-assembling systems (micellar liquid crystals) within the framework of a hard-particle model. The discotic system consists of a set of reversibly assembled polydisperse right cylindrical discs. The monomer unit was a symmetric right cylinder and a free energy of association of  $-\phi(T)k_B T$  was assigned to each monomer-monomer contact. Using a scaled particle treatment of fluid configurational entropy and a cell description of periodic columnar density modulation they obtained a phase diagram which has many features in common with the experimental phase diagram for the CsPFO/water<sup>1,2,19</sup> and APFO/water<sup>3</sup> systems. In particular the inclusion of polydispersity in the model is sufficient to suppress columnar ordering<sup>17</sup> and favoured a translationally ordered smectic phase at high particle volume fractions. The volume fraction dependence of the orientational order parameters and average disc axial ratios were also calculated for a series of temperatures ( $\phi^{-1}$ ) chosen so that the values of these parameters at the phase transitions could be obtained and tested against experiment.

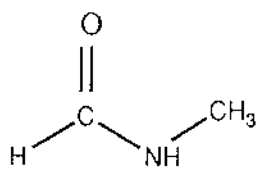
It has been shown that the addition of the co-surfactant perfluorooctanol to the CsPFO/H<sub>2</sub>O system leads to larger micelles<sup>20</sup>. The long chain surfactant molecules form part of the micelles and lead to a reduction in the electrostatic repulsion between the carboxylate head groups. The addition of electrolyte also leads to larger micelles<sup>21,22</sup> by influencing the self assembly of the surfactant molecules.

The object of this study is to determine the phase behaviour for the CsPFO/D<sub>2</sub>O system upon the addition of the four co-solvents formamide (FA), *N*-methylformamide (NMF), *N,N*-dimethylformamide (DMF), and *N,N*-dimethylacetamide (DMA) using <sup>2</sup>H and <sup>133</sup>Cs NMR spectroscopy to determine the phase transition temperatures. The phase behaviour of these systems will be compared to that of the binary CsPFO/D<sub>2</sub>O system<sup>1</sup> to examine how the co-solvent effects the phase behaviour in terms of the self assembly of the discotic micelles. It is well known that the simple amides FA, NMF, DMF and DMA are of interest as model compounds in biochemistry. They are of interest here because they represent, in the given sequence, a transition from a small, hydrogen-bonding, protic solvent with no hydrophobic groups (FA) to a large, aprotic

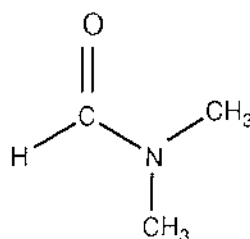
solvent with three methyl groups (DMA). The number of methyl groups in a molecule is known to strongly affect structural and dynamic properties of aqueous mixtures of these molecules. The range they exhibit in their physical properties (such as relative permittivity and surface tension) is of particular interest.



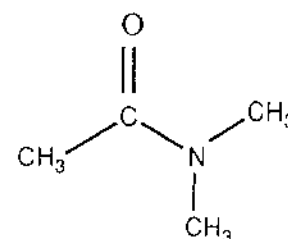
FORMAMIDE



N-METHYL FORMAMIDE



N,N-DIMETHYL FORMAMIDE



N,N-DIMETHYL ACETAMIDE

In all the experiments the CsPFO to D<sub>2</sub>O ratio is kept constant and small amounts of co-solvent are added such that the phase behaviour of the binary CsPFO/D<sub>2</sub>O system is essentially preserved. It will be shown that the mechanism for the phase transitions is essentially a hard particle one and it is the self assembly which determines the phase behaviour.



## 2. Experimental.

### 2.1 Chemicals.

N,N-dimethyl formamide and N,N-dimethyl acetamide (BDH AnalaR grade) were dried over calcium hydride and distilled under vacuum. N-methyl formamide (Aldrich) was of the highest purity available (99%) and used without further purification. Formamide (BDH AnalaR grade) was dried over anhydrous sodium sulphate and distilled under vacuum. N,N-dimethyl formamide-*d*<sub>7</sub> (99.5 atom % D) and deuterium oxide (99.9 atom % D) (both from Aldrich) were used without further purification. The above solvents are all hygroscopic hence were stored under dry nitrogen in a dessicator.

Caesium pentadecafluorooctanoate (CsPFO) was made by neutralising the sparingly soluble parent acid (Aldrich) with caesium carbonate (Reidel-de Haen) in deionized and doubly distilled water. The slightly alkaline solution was tested with litmus paper (BDH) then freeze-dried. The pure CsPFO salt was obtained by double recrystallisation from 50% butanol/hexane. Residual solvent was removed by prolonged heating (at least 24 hours at 50 °C) under vacuum. The pure crystals appeared waxy and pure white. CsPFO is hygroscopic so was also kept in a dessicator.

A hazard sheet for handling these chemicals is included in Appendix 2

### 2.2 Sample Preparation.

#### 2.2.1 NMR Sample Preparation.;

Samples were prepared to give a constant CsPFO to D<sub>2</sub>O mass ratio with varying amount of amide in the following way. Stock solutions of CsPFO in D<sub>2</sub>O were gravimetrically prepared using a Mettler AT 261 Delta Range five-figure balance. CsPFO was added by funnel to a 10 ml ampoule. The mass of D<sub>2</sub>O required to make up the desired salt mass fraction ( $w=0.4$  or  $0.5$ ) was calculated and added by long hypodermic syringe. The ampoule was flame sealed and the solution thoroughly mixed. Care was taken not to contaminate the ampoule neck during weighing to prevent evaporation of D<sub>2</sub>O or decomposition of salt during sealing. Samples prepared in this manner varied in composition to within  $\pm 0.002$  mass fraction.

The stock solution was heated into the isotropic phase and thoroughly mixed. A sample was prepared by first adding a 0.6 ml aliquot of the stock solution by syringe into a preweighed 5 mm o.d. NMR tube that had been cleaned with concentrated nitric acid, thoroughly washed with deionized doubly distilled water and dried in an oven at

80 °C. The mass of stock solution in the NMR tube was then determined and this was used to calculate the approximate volume of amide required. The amide was added to the NMR tube in a fume cupboard using a glass syringe. The stoppered solutions were reweighed then flame sealed. During the course of the work presented here it was necessary to prepare several stock CsPFO/D<sub>2</sub>O solutions. A control sample (no amide added) was thus retained from every batch and the I-to-N<sub>D</sub><sup>+</sup> phase transition temperature determined to ensure uniform stock solution concentration. Thorough mixing of the samples in the isotropic phase was performed prior to use.

### 2.2.2 Conductivity Sample Preparation.

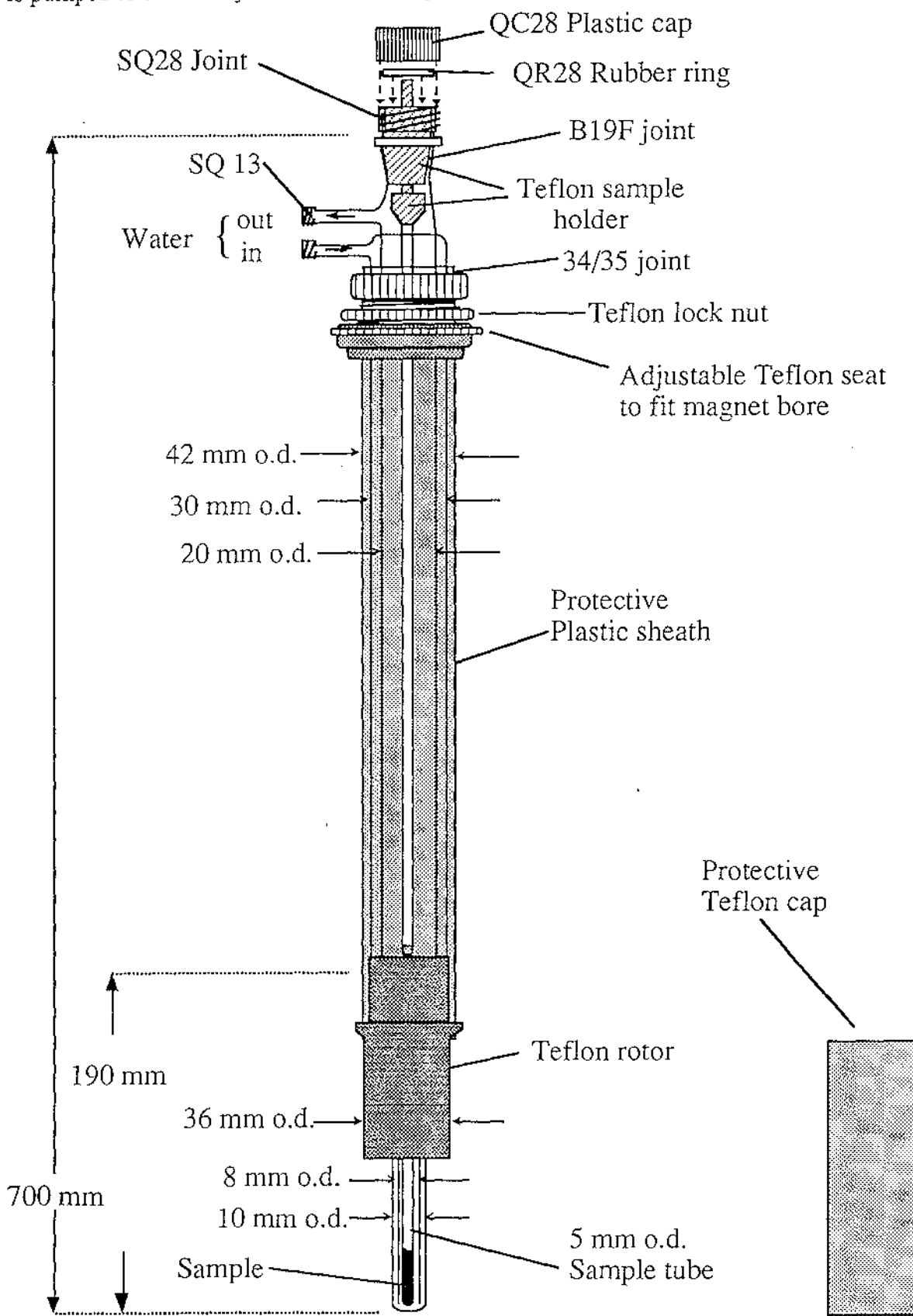
Stock D<sub>2</sub>O/amide solvent solutions were gravimetrically prepared in 25 cm<sup>3</sup> volumetric flasks (in a fume cupboard) such that the mole fraction of amide in D<sub>2</sub>O was 0.0231 (corresponding to approximately 5% by mass formamide in D<sub>2</sub>O). Standard solutions of approximately 0.1 mol kg<sup>-1</sup> CsPFO in these solvents were made up in 10 cm<sup>3</sup> volumetric flasks. After the conductivity of a solution had been measured, most of the analyte was recovered and reweighed. This was then diluted by a known mass of solvent and the new amphiphile concentration calculated. This process was repeated until the CMC had been defined.

## 2.3 Instrumentation.

### 2.3.1 Temperature control.

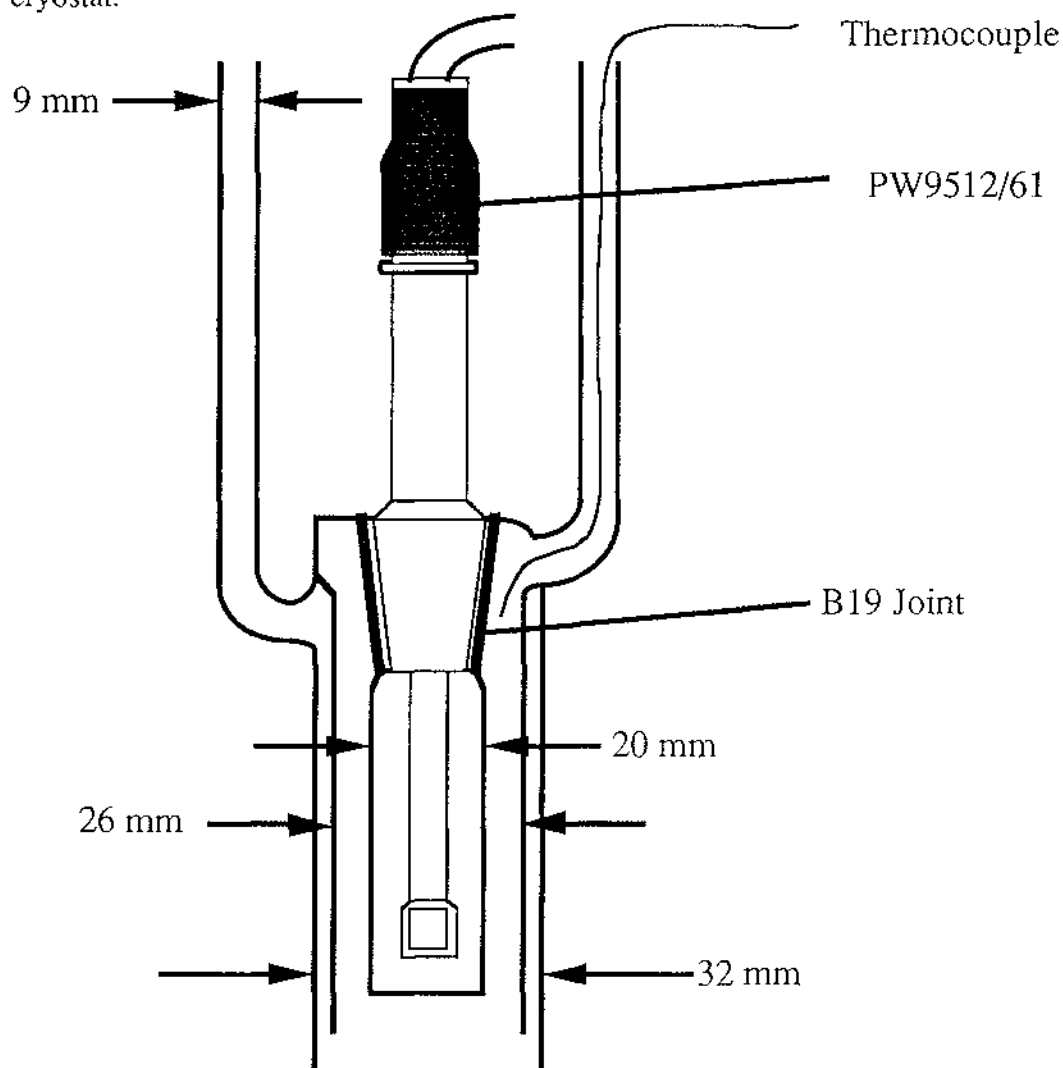
Precise, stable and accurate temperature control is fundamental to the determination of phase transition temperatures. It will be seen that both <sup>2</sup>H and <sup>133</sup>Cs quadrupole splittings are strongly temperature dependent. The JEOL JNM-GX270 NMR spectrometer is supplied with an air flow temperature control system. The use of air, with its low heat capacity, only allows temperatures stable to ± 0.1 K and gives rise to thermal gradients along the sample. This leads to sample inhomogeneity through solvent distillation and phase separation which manifests itself as a broadening of NMR spectrum lines. A double-pass water flow sample cell has been developed<sup>23</sup> (and recently modified) (figure 2.1) which, when coupled to a Colora WK3 cryostat gives temperature control to within ± 5 mK over several hours and which has been shown to produce samples with exceptional temperature and concentration homogeneity.

**Figure 2.1** Double-pass water flow sample cell used to control the sample temperature during NMR experiments using a JEOL GX270 spectrometer. The Teflon rotor is the standard 10 mm sample spinner supplied by the spectrometer manufacturer. The water is pumped to the cell by a Colora WK3 cryostat.



Temperature control during conductivity measurements is also important so a double-pass water flow cell (figure 2.2) was designed and temperature control achieved by using a Colora WK3 cryostat as for the NMR experiments.

Figure 2.2 Double-pass water flow sample cell used to control the sample temperature during conductivity experiments. The water is pumped to the cell by a Colora WK3 cryostat.



### 2.3.2 Temperature Measurement.

Temperature was continuously monitored during both the NMR and conductivity measurements by the insertion of a copper/constantin thermocouple into the water flow close to the sample. The potential between this and a reference thermocouple maintained at 0 °C by immersion in an ice slurry was measured to an accuracy of 0.1  $\mu$ V using a Philips PM2535 systems multimeter. The thermocouple had been calibrated at 2 K intervals to an accuracy and precision of  $\pm 1$  mK against a

Hewlett-Packard 2804A digital quartz thermometer with a 2805A temperature probe. The potential was converted to temperature by linear interpolation between calibration points using a program written on MathCAD.

### 2.3.3 NMR Instrumentation.

A JEOL JNM-GX270 spectrometer with an Oxford Instruments 6.34 Tesla wide bore superconducting magnet was used to observe  $^2\text{H}$  and  $^{133}\text{Cs}$  nuclei using an NM-G2710 10mm tuneable probe.

The probe was tuned to the  $^{133}\text{Cs}$  frequency giving a  $\pi/2$  pulse width of 19  $\mu\text{s}$  and a consequent effective spectral frequency range of about 50 kHz. A typical  $^{133}\text{Cs}$  spectral frequency range was 30 kHz.  $^2\text{H}$  spectra were recorded without retuning the probe so that consecutive  $^{133}\text{Cs}$  and  $^2\text{H}$  spectra could be obtained without delay. The  $^2\text{H}$   $\pi/2$  pulse when the probe was tuned to the  $^{133}\text{Cs}$  frequency was 400  $\mu\text{s}$  and a  $\pi/4$  pulse of 200  $\mu\text{s}$  was used for spectral accumulation, giving an effective spectral range of about 5 kHz. This spectral range was more than adequate for all  $^2\text{H}$  spectra where typical quadrupole splittings ranged from 200 Hz to 1 kHz. For the  $^{133}\text{Cs}$  counterion measurements and the  $^2\text{H}$  NMR of heavy water the FID was collected immediately following a  $\pi/2$  pulse.

Typical acquisition parameters are shown in table 2.1.

**Table 2.1.** Typical NMR acquisition parameters.

Nucleus	$^2\text{H}$	$^{133}\text{Cs}$
Experiment Mode	Single Pulse- Non decoupled	Single Pulse- Non decoupled
Observation Frequency	41.47 MHz	35.31 MHz
Sweep Width	2 kHz	10-60 kHz
Data Points	8192	32768
Broadening Factor	0.1 Hz	1 Hz
Accumulations	4	16
Pulse Width	200 $\mu\text{s}$	19 $\mu\text{s}$
Pulse Delay	2 s	0.5 s

#### 2.3.4 Conductivity Instrumentation.

The cell constant of a Philips PW9512/61 conductivity cell was determined at 298 K using a standard 0.100 mol l<sup>-1</sup> KCl solution and found to be 0.725 cm<sup>-1</sup>. This cell, attached to a Philips PW9509 digital conductivity meter, was then used to measure conductivities of samples at a measuring frequency of 2000 Hz, the highest frequency available on the PW9509 meter.